ESTIMATION OF GAS PERMEABILITIES FOR THE MARICOPA SITE, ARIZONA

Final Report

by

Bridget R. Scanlon

Edward Angle

Jinhuo Liang

Robert Reedy

Bureau of Economic Geology, The University of Texas at Austin, Noel Tyler, Director

August, 1998

INTRODUCTION

Upward and downward migration of gases from waste-disposal facilities is a critical issue for low-level radioactive waste disposal. Gaseous radionuclides in low-level waste include H-3, C-14, and Rn-222. Upward migration of gases to the surface can be important, particularly during operation of the facility (Kozak and Olague, 1994). High tritium values (for example 1,100 TU at 24 m depth, ≤ 162 TU at 109 m depth) have been found adjacent to the Beatty site, Nevada, that cannot readily be explained by liquid or combined liquid and vapor transport (Prudic and Striegl, 1995; Striegl et al., 1996). Because disposal practices at Beatty varied in the past and included disposal of as much as ~ 2,000 m^3 of liquid waste, further research in tritium movement at Beatty is warranted. Transport mechanisms for gases include not only diffusion but also advection. Analysis of gas transport is important at many low-level waste disposal facilities as shown by the intensive program to monitor concentrations and concentration gradients of gaseous radionuclides proposed for the California low-level radioactive waste disposal facility (Harding Lawson & Assoc., 1991). Performance assessment calculations require information on parameters related to gas transport to predict long-term migration of gases in the subsurface. The purpose of this study is to evaluate different techniques of estimating gas transport parameters and monitoring subsurface gas migration.

The objective of this study is to examine different techniques for evaluating gas permeability. Pneumatic pressure tests will be conducted to estimate vertical and horizontal air permeabilities at different levels. In addition, permeabilities will be calculated from atmospheric breathing data that will include evaluation of subsurface response to barometric pressure fluctuations. Computer simulations suggest that air from the surface can move several meters into the ground during typical barometric pressure cycles (Massmann and Farrier, 1992). Gas ports will be installed at different depths in two boreholes to evaluate atmospheric pumping. The results of this study will provide valuable information on subsurface gas transport processes and the

various techniques to obtain data on parameters required for simulation of such processes. These data will be required for performance assessment calculations.

METHODS

Theory

Advective transport of gases depends on gas permeability and pressure gradient. Gas permeability can be estimated from (1) pneumatic tests and (2) analysis of atmospheric pumping data.

Pneumatic Tests

Pneumatic tests are widely used to evaluate gas permeability in the unsaturated zone. In pneumatic tests, air is either injected or extracted from a well, and pressure is monitored in gas ports installed at different depths in surrounding monitoring wells. Most analyses of pneumatic tests assume that the gas content (θ_G) is constant over time; that is, that there is no redistribution of water during the test.

A variety of techniques are available for analyzing pneumatic tests. The initial transient phase of the test or the steady-state portion of the test can be analyzed. The transient phase of gas tests is generally short (~ seconds to hours; Edwards, 1994) and it is sometimes difficult to collect reliable data. Most studies analyze the steady-state portion of the test. Analysis of pneumatic tests is similar to the inverse problem in well hydraulics, where gas permeabilities are estimated from pressure data. Various solutions for estimating gas permeability differ in terms of the boundary conditions that are assumed at the ground surface (such as unconfined, leaky confined, and confined) and the method of solution. The lower boundary is generally assumed to be the water table or an impermeable layer. All solutions assume radial flow to a vertical well. Steady-state and horizontally axisymmetric air flow in the unsaturated zone is described by the following equation:

$$k_r \frac{\partial^2 \phi}{\partial r^2} + \frac{k_r}{r} \frac{\partial \phi}{\partial r} + k_z \frac{\partial^2 \phi}{\partial z^2} = 0 \qquad (1)$$

where k_r is radial permeability, r is radial distance, z is depth, and $\phi = P^2$. Baehr and Hult (1991) provided analytical solutions to this equation. A computer code (AIR2D) is available that includes these analytical solutions (Joss and Baehr, 1997). Air compressibility is approximated by the ideal gas law. The pressure dependence of permeability (Klinkenberg effect) is neglected.

Analysis of Atmospheric Pumping Data

Comparison of temporal variations in gas pressure (monitored at different depths in the unsaturated zone) with atmospheric pressure fluctuations at the surface can be used to determine the minimum vertical air permeability between land surface and monitoring depth (Weeks, 1978; Nilson et al., 1991).

Data analysis consists of expressing the variations in atmospheric pressure as time-harmonic functions. Attenuation of the surface waves at different depths in the unsaturated zone provides information on how well or how poorly the unsaturated sections are connected to the surface. The accuracy of the results increases with the amplitude of the surface signals.

The governing equation is

$$\frac{\partial P}{\partial t} = \alpha \frac{\partial^2 P}{\partial z^2} \tag{2}$$

where P is pressure, t is time, $\alpha = \dfrac{kP_0}{\mu_G \theta_G}$ is the pneumatic diffusivity, k is permeability, P_0 is the mean static pressure, μ_G is the gas viscosity, and θ_G is volumetric gas content. The surface pressure varies harmonically as

$$P = P_o + \Delta P \cos \omega t \tag{3}$$

where ω is the angular frequency ($2\pi/T$) and T is the period. The water table or a low-permeability air barrier is assumed to act as a no-flow boundary. Equation 2 is solved with the above boundary conditions for the ratio of subsurface to surface pressure amplitudes (Carslaw and Jaeger, 1959 in [Nilson et al, 1991]):

$$\frac{P - P_0}{\Delta P} = \frac{\sqrt{\cosh\left[\sqrt{2}\lambda\left(1 - \dfrac{z}{h}\right)\right] + \cos\left[\sqrt{2}\lambda\left(1 - \dfrac{z}{h}\right)\right]}}{\sqrt{\cosh\sqrt{2}\lambda + \cos\sqrt{2}\lambda}} \tag{4}$$

where $\frac{P - P_0}{\Delta P}$ is the amplitude ratio, ΔP is the pressure variation at the surface, P is the pressure at depth, P_0 is the mean pressure at the mean surface, $\lambda = h\sqrt{\frac{\omega}{\alpha}} = \sqrt{\frac{2\pi h^2}{\alpha T}}$, and h is the depth to the lower boundary or water table. Using equation 4 we solve for λ, then calculate α and k. The ratio of the amplitude at a certain depth z compared with the amplitude at the surface can be obtained graphically or by using time series analysis (Rojstaczer, 1995).

Materials and Methods

A total of six boreholes were drilled for soil gas studies at the Maricopa site. Four boreholes were drilled outside the irrigated plot for pneumatic pressure tests. The other two boreholes were used to monitor subsurface gas pressures in response to barometric pressure fluctuations, one inside (MAM1) and the other outside (MAM2) the irrigated plot.

Four boreholes were drilled to conduct pneumatic pressure tests. An injection/extraction borehole (designated MI1) was drilled to 5 m depth and 3 monitoring boreholes (designated MP1, MP2, and MP4) to 10 m depth at distances of 1, 2, and 4 m from the injection/extraction borehole. Sediment samples were collected at 0.3 m intervals to total depth for texture and water content analyses in all boreholes. A PVC screen (5 cm diameter with 0.25 mm slots) was installed at the base of the injection/extraction well (MI1). A PVC pipe of similar diameter was used to connect the screen to the surface. Sand (20/40) was used to complete the boreholes around the screens and the remainder of the borehole was completed with grout to land surface. Gas ports were installed at 2.5 m intervals in each of the monitoring boreholes. The gas ports consisted of 3 mm copper tubing at the desired test depth with a 3 cm slotted section at the base. Thermistors were placed at each depth in MP2 to record temperature fluctuations during testing.

The pneumatic tests were conducted using a high volume, low pressure blower to inject/extract air into MI1. A ROTRON Model EN6F5L blower was used with a 1.80 m section of flexible hose (5 cm diameter) attached to a 3 m section of pipe to establish laminar flow. At the end of the pipe a thermistor, an Omega flow meter, and a 15 psi pressure transducer were used to

measure the air temperature, flow rate, and injection pressure respectively. A second section of flexible hose connected the pipe to the PVC well head on MI1. A Campbell CR10X data logger was used to monitor pressures and temperatures. A Campbell AM416 Multiplexer was used to switch between the 12 pressure transducers and 4 thermistors used during testing. Data required for analysis included flow rate from the air pump, temperature and pressure of injected or extracted air, pressure at all monitored depths in all monitored boreholes, and temperature measurements from one borehole. Injection tests were conducted at 5, 10, and 15 Pa. Two tests were run at each injection pressure. Each test was run until no observable change occurred in the farthermost pressure transducer (MP4, 10 m depth).

The monitoring boreholes were drilled using a hollow stem auger (diameter: 17.8 cm [7 inch]) to a depth of 11 m. Soil samples were collected at 0.3 m depth intervals for analysis of texture and water content. Bulk density samples were collected at 0.9 to 1.5 m depth intervals. Gas ports, consisting of slotted stainless steel screens (2.54 cm outside diameter, 30 cm long), were installed at 2.5 m intervals to 10 m. A YSI thermistor was installed with each gas port to monitor temperature change at depth. The gas ports were connected to the surface using nylon tubing (0.635 cm outside diameter). The borehole was backfilled with sand 13 cm below and above the screens and a 50:50 sand/bentonite mixture to form a seal and to prevent preferential flow in the borehole.

The data logging system consisted of a Campbell Scientific CR10X data logger that controlled solenoid valves, a pressure transducer, a barometer, and thermistors. Each gas port was connected to a dedicated solenoid valve. An extra solenoid valve was included to use as an atmospheric vent. The solenoid controlled flow to a common manifold measured with a single differential pressure transducer (Model 239, SETRA, Acton, MA) at the surface. The solenoid valves were opened and closed by a Campbell CD16AC switching unit which received commands from the CR10X. A Setra 270 Barometer was included to monitor barometric pressure fluctuations. Surface and subsurface gas pressures and temperatures were logged every 15 min to evaluate attenuation and phase lag of pressure fluctuations with depth.

RESULTS AND DISCUSSION

Soil Texture and Water Content

Soil texture is coarse grained (Figure 1, Table 1). Gravel content ranged from 0 to 37%. High gravel content was found generally at depths > 5 m in all MP profiles. Mean sand content ranged from 71 to 79%. The dominant textures ranged from gravely sand, sand, loamy sand, and sandy loam. Water content ranged from 0.03 to 0.34 g g^{-1}. Mean water contents ranged from 0.08 to 0.12 g g^{-1} in the various profiles. There was no systematic variation in water content with depth. Variations in water content were generally not related to textural variations.

Pneumatic Tests

Pneumatic tests were conducted in February 1998. The relative locations of the injection and monitoring wells are shown in Figure 2. we monitored the flow rate, pressure, and temperature of the air at the well head, and subsurface pressures at 2.5 m depth intervals in 3 monitoring wells at distances of 1 m (MP1), 2 m (MP2) and 4 (MP4) from the injection well and temperatures at the monitoring well. Results from a typical pneumatic test are shown in Figure 3. The initial small step increase in injection pressure (a) corresponds to the pump being switched on and the second step increase (b) corresponds to connection of the pump to the well. Pressures were highest at 5 m depth which corresponds to the injection depth and decreased with distance from the injection well. Pressures at all other monitoring points were much lower. The transient portion of the tests was very short (~ minutes). The steady state data were analyzed using the analytical solutions in the AIR2D code (Baehr and Hult, 1991). The upper boundary was assumed to be open to the atmosphere and the lower boundary is the water table at 11.2 m depth. Input data for the AIR2D simulations are presented in Table 2. Results of the analyses indicate that the horizontal permeability ranged from 4.8 to 6.7 x10^{-12} m^2 (4.2 to 7.2 darcies, Table 3). Results from duplicate tests conducted at similar injection pressures were similar. The vertical permeability

ranged from 1.2 to 1.8 x 10^{-12} m^2 and was 2 to 3 times less than the horizontal permeability. The permeability anisotropy is attributed to layering of the sediments.

Atmospheric Pumping

The maximum pressure variation recorded at the surface was 1,000 Pa (10 mbar) in a 24 hr period (Figure 4). This surface pressure variation was attenuated with depth. During high atmospheric pressure periods, the differential pressure at depth is negative, meaning a lower pressure at depth and during low atmospheric pressure periods differential pressure is positive, meaning a higher pressure at depth. Equation 4 was used to solve for permeability. The amplitude of the pressure variation at the surface (ΔP) was equal to 500 Pa and at different depths ranged from 489 to 497 Pa. The maximum differential pressures measured at the different depths ranged from 3 to 11 Pa for this period which approaches the limits of the differential pressure transducer used to monitor these pressure fluctuations (Figure 5). Because attenuation of the pressure signal with depth was negligible, the amplitude ratio is close to 1. Equation 4 was solved iteratively, and λ was estimated by minimizing the difference between the measured and calculated amplitude ratio. In order to calculate permeability from λ a value of 0.2 was used for volumetric air content. Minimum vertical air permeabilities ranged from 0.6 to 0.9 x10^{-12} m^2 (0.6 to 0.9 darcies) at different depths. These values of vertical permeability are similar to vertical air permeabilities estimated from the pneumatic data.

Sensitivity analyses were conducted to evaluate the atmospheric pumping technique for estimation of minimum vertical air permeabilities under different conditions. Variations in the ratio of the subsurface to the surface P amplitudes for different permeabilities and water table depths were calculated by modifying equation 4. A ratio of 1 indicates no pressure attenuation. These analyses indicate that the attenuation factor is negligible in high permeability media if the water table is shallow (~ 10 m; Figure 6a). Decreasing the permeability increases the pressure attenuation. Increasing the depth to the water table also increases the pressure attenuation. The

combination of high permeability and shallow water table at this site results in negligible attenuation of barometric pressure fluctuations with depth.

CONCLUSIONS

The site is characterized by coarse grained sediments with mean water contents of ~ 0.1 g g^{-1}. Pneumatic tests resulted in horizontal permeabilities that ranged from 1 to 2 x 10^{-12} m^2. Horizontal permeabilities exceeded vertical permeabilities by a factor of 2 to 3 which is consistent with the layering of the sediments at this site. Vertical permeabilities estimated from atmospheric pumping data were similar to those calculated from the pneumatic tests. The high permeabilities and shallow water table at this site result in negligible attenuation of surface pressure fluctuations with depth which is consistent with theory.

REFERENCES

Baehr, A. L., and M. F. Hult, Evaluation of unsaturated zone air permeability through pneumatic tests, *Water Resour. Res., 27*, 2605-2617, 1991.

Carslaw, H. S., and J. C. Jaeger, The Conduction of Heat in Solids, pp. 510, Oxford Univ. Press, London, 1959.

Edwards, K. B., Air permeability from pneumatic tests in oxidized till, *J. Environ. Engin., 120*(2), 329-346, 1994.

Folk, R. L., Petrology of sedimentary rocks, pp. 182, Hemphill, Austin, Texas, 1974.

Harding Lawson & Associates, 1991, Final vadose zone and trench cap monitoring plan: proposed low-level radioactive waste disposal facility, Ward Valley, California.

Joss, C. J., and A. L. Baehr, AIR2D - A computer program to simulate two dimensional axisymmetric air flow in the unsaturated zone, in *U.S. Geol. Survey Open File Report 97-588*, pp. 106, U.S. Geol. Survey, 1997.

Kozak, M.W. and Olague, N.E., 1993, Updated recommendations for low-level waste performance assessment, Proceedings of the Symposium on Waste Management at Tucson, Arizona, 1993, 371-376.

Kreamer, D.K., Weeks, E.P., Thompson, G.M., 1988, A field technique to measure the tortuosity and sorption-affected porosity for gaseous diffusion of materials in the unsaturated zone with experimental results from near Barnwell, South Carolina, Water Resour. Res., 24, 331-341.

Massmann, J., and Farrier, D.F., 1992, Effects of atmospheric pressures on gas transport in the vadose zone: Water Resources Research, v. 28, 777-791.

Nilson, R. H., E. W. Peterson, K. H. Lie, N. R. Burkard, and J. R. Hearst, Atmospheric pumping: a mechanism causing vertical transport of contaminated gases through fractured permeable media, *J. Geophys. Res., 96(B13)*, 21933-21948, 1991.

Prudic, D. E., and R. G. Striegl, Tritium and radioactive Carbon (14C) analyses of gas collected from unsaturated sediments next to a low-level radioactive-waste burial site south of Beatty, Nevada, April 1994 and July 1995, in *U.S. Geol. Surv. Open-File Report*, pp. 7, U.S. Geol. Surv., 1995.

Rojstaczer, S., and J. P. Tunks, Field-based determination of air diffusivity using soil-air and atmospheric pressure time series, *Water Resour. Res., 12,* 3337-3343, 1995.

U.S. Dept. of Agriculture, 1975, Soil taxonomy: Washington, D.C., Soil Conservation Service, 754 p.

Striegl, R. G., D. E. Prudic, J. S. Duval, R. W. Healy, E. R. Landa, D. W. Pollock, D. C. Thorstenson, and E. P. Weeks, Factors affecting tritium and 14Carbon distributions in the unsaturated zone near the low-level radioactive-waste burial site south of Beatty, Nevada, in *U.S. Geological Survey Open File Report*, pp. 16, U.S. Geological Survey, 1996.

Weeks, E. P., Field determination of vertical permeability to air in the unsaturated zone, in *U.S. G.S. Prof. Paper*, pp. 41, U.S. Geol. Surv., 1978.

Table 1. Gravimetric water content, gravel, sand, silt and clay contents and soil textural classification

Well ID	Depth (m)	θ_g	Gravel (%)	Sand (%)	Silt (%)	Clay (%)	Soil Texture
MI1	0.34	0.05	2	67	15	16	SANDY LOAM
	0.85	0.08	2	64	19	16	SANDY LOAM
	1.52	0.11	1	66	26	8	SANDY LOAM
	2.87	0.11	0	85	11	4	LOAMY SAND
	3.08	0.11	3	82	11	5	LOAMY SAND
	3.32	0.11	0	84	12	5	LOAMY SAND
	3.69	0.13	0	89	6	5	SAND
	3.99	0.11	29	57	11	4	GRAVELLY MUDDY SAND
	4.33	0.10	2	64	19	16	SANDY LOAM
	4.57	0.10	3	65	18	15	SANDY LOAM
	4.79	0.10	1	64	28	7	SANDY LOAM
	5.15	0.18	0	64	29	7	SANDY LOAM
	Average	0.11	4	71	17	9	
MP1	0.24	0.03	3	68	18	13	SANDY LOAM
	0.88	0.09	1	62	22	15	SANDY LOAM
	1.19	0.10	2	67	28	4	SANDY LOAM
	1.46	0.08	11	64	18	7	GRAVELLY MUDDY SAND
	1.80	0.07	0	82	14	4	LOAMY SAND
	1.89	0.07	0	93	6	1	SAND
	2.16	0.05	0	88	9	3	SAND
	2.35	0.06	0	54	40	6	SANDY LOAM
	2.71	0.10	0	84	12	4	LOAMY SAND
	3.05	0.12	0	73	23	4	SANDY LOAM
	3.28	0.09	0	69	26	5	SANDY LOAM
	3.63	0.12	1	91	7	1	SAND
	3.99	0.13	3	92	5	1	SAND
	4.19	0.09	1	92	6	1	SAND
	4.54	0.09	3	90	6	2	SAND
	4.91	0.13	10	87	2	1	GRAVELLY SAND
	5.18	0.08	12	86	1	1	GRAVELLY SAND
	5.70	0.21	19	77	3	2	GRAVELLY SAND
	6.37	0.24	15	82	3	1	GRAVELLY SAND
	6.74	0.07	14	79	6	2	GRAVELLY SAND
	7.04	0.06	14	82	3	2	GRAVELLY SAND
	7.35	0.04	36	60	3	2	SANDY GRAVEL
	7.35	0.05	10	82	5	4	GRAVELLY SAND
	7.65	0.04	1	67	21	12	SANDY LOAM
	8.46	0.03	3	79	12	7	LOAMY SAND
	8.81	0.04	11	75	10	5	GRAVELLY MUDDY SAND
	9.17	0.05	7	80	8	5	GRAVELLY MUDDY SAND
	9.37	0.06	31	60	6	4	MUDDY SANDY GRAVEL
	9.68	0.04	37	56	6	2	MUDDY SANDY GRAVEL
	9.78	0.03	0	67	29	4	SANDY LOAM
	10.09	0.06	0	63	31	6	SANDY LOAM
	Average	0.08	8	76	12	4	
MP2	0.34	0.06	1	70	16	14	SANDY LOAM
	0.63	0.05	2	66	19	14	SANDY LOAM
	0.94	0.08	2	67	21	11	SANDY LOAM
	1.12	0.08	2	49	40	10	LOAM

Table 1. Gravimetric water content, gravel, sand, silt and clay contents and soil textural classification

Well ID	Depth (m)	θ_g	Gravel (%)	Sand (%)	Silt (%)	Clay (%)	Soil Texture
MP2	1.49	0.08	4	64	28	5	SANDY LOAM
	1.86	0.06	0	78	16	6	LOAMY SAND
	2.16	0.06	1	70	20	10	SANDY LOAM
	2.41	0.05	0	84	11	5	LOAMY SAND
	2.47	0.04	0	87	10	4	LOAMY SAND
	2.71	0.04	0	82	15	3	LOAMY SAND
	3.08	0.15	0	67	29	4	SANDY LOAM
	3.28	0.15	0	84	14	2	LOAMY SAND
	3.63	0.12	1	94	3	2	SAND
	3.89	0.12	6	90	3	1	GRAVELLY SAND
	4.54	0.11	6	94	-1	0	GRAVELLY SAND
	4.60	0.11	4	93	2	2	SAND
	5.21	0.12	8	82	8	2	GRAVELLY MUDDY SAND
	6.45	0.15	10	89	1	0	GRAVELLY SAND
	6.74	0.34	9	86	5	1	GRAVELLY SAND
	6.93	0.12	0	94	5	1	SAND
	7.24	0.05	26	70	3	1	GRAVELLY SAND
	7.35	0.06	27	70	2	1	GRAVELLY SAND
	7.65	0.04	17	76	5	3	GRAVELLY SAND
	7.85	0.02	16	77	5	2	GRAVELLY SAND
	8.15	0.11	1	66	22	11	SANDY LOAM
	8.56	0.04	3	62	21	14	SANDY LOAM
	8.90	0.04	2	79	13	7	LOAMY SAND
	9.17	0.07	15	70	9	6	GRAVELLY MUDDY SAND
	9.48	0.06	13	79	4	4	GRAVELLY SAND
	9.68	0.05	27	67	3	3	GRAVELLY SAND
	10.03	0.05	18	75	4	4	GRAVELLY SAND
	10.39	0.04	0	53	38	9	SANDY LOAM
	Average	0.08	7	76	12	5	
MP4	0.53	0.07	3	67	20	11	SANDY LOAM
	0.88	0.09	1	66	20	14	SANDY LOAM
	1.45	0.12	3	74	17	7	SANDY LOAM
	1.49	0.10	0	65	22	13	SANDY LOAM
	2.36	0.05	5	86	7	3	SAND
	2.71	0.14	0	74	19	7	SANDY LOAM
	3.41	0.09	0	70	24	6	SANDY LOAM
	4.24	0.11	0	62	34	4	SANDY LOAM
	5.21	0.10	0	91	7	1	SAND
	6.02	0.18	5	91	2	2	GRAVELLY SAND
	6.31	0.10	4	70	23	4	SANDY LOAM
	6.92	0.22	9	77	9	6	GRAVELLY MUDDY SAND
	7.28	0.07	0	92	6	2	SAND
	7.85	0.04	21	76	3	1	GRAVELLY SAND
	8.20	0.04	12	79	7	3	GRAVELLY MUDDY SAND
	8.76	0.11	0	59	27	14	SANDY LOAM
	9.07	0.07	0	65	24	11	SANDY LOAM
	9.68	0.04	8	84	5	4	GRAVELLY SAND
	9.98	0.07	10	57	26	7	GRAVELLY MUDDY SAND
	Average	0.10	4	74	16	6	

Table 1. Gravimetric water content, gravel, sand, silt and clay contents and soil textural classification

Well ID	Depth (m)	θ_g	Gravel (%)	Sand (%)	Silt (%)	Clay (%)	Soil Texture
MAM1	0.53	0.05	2	64	18	17	SANDY LOAM
	0.88	0.11	1	58	24	18	SANDY LOAM
	1.55	0.12	6	81	4	9	GRAVELLY MUDDY SAND
	2.35	0.09	30	64	4	2	GRAVELLY SAND
	2.62	0.03	0	69	24	7	SANDY LOAM
	3.22	0.06	19	67	11	3	GRAVELLY MUDDY SAND
	4.30	0.05	0	56	36	8	SANDY LOAM
	5.14	0.13	2	90	7	2	SAND
	6.13	0.15	3	93	3	1	SAND
	7.28	0.26	0	61	34	5	SANDY LOAM
	7.83	0.07	0	95	4	1	SAND
	8.15	0.05	7	90	2	1	GRAVELLY SAND
	8.76	0.27	0	61	20	19	SANDY LOAM
	9.07	0.06	2	78	11	10	SANDY LOAM
	9.78	0.04	14	82	1	3	GRAVELLY SAND
	Average	0.10	6	74	13	7	
MAM2	0.64	0.07	2	63	17	19	SANDY LOAM
	1.45	0.10	24	63	7	7	GRAVELLY MUDDY SAND
	1.75	0.10	0	86	10	4	LOAMY SAND
	2.36	0.07	0	96	2	1	SAND
	2.67	0.09	0	75	20	5	LOAMY SAND
	3.38	0.08	0	76	19	4	LOAMY SAND
	4.24	0.11	0	88	7	4	SAND
	5.21	0.09	19	78	2	2	GRAVELLY SAND
	6.08	0.16	1	95	2	3	SAND
	6.93	0.15	25	72	2	1	GRAVELLY SAND
	7.24	0.08	2	87	5	6	SAND
	7.85	0.04	0	94	3	3	SAND
	8.15	0.04	22	73	3	2	GRAVELLY SAND
	8.76	0.05	1	77	12	11	SANDY LOAM
	9.07	0.09	1	72	18	10	SANDY LOAM
	9.72	0.05	12	65	11	12	GRAVELLY MUDDY SAND
	10.12	0.05	9	76	8	6	GRAVELLY MUDDY SAND
	Average	0.08	7	79	9	6	

Table 2. Input data for air permeability estimation using AIR2D.

Extraction air pressure (kPa)	5	5	10	10	15	15	20	20
Number of pressure transducers	12	12	12	12	12	12	12	12
Air temperature (°C)	20	20	20	20	20	20	20	20
Soil temperature (°C)	27.4	28.1	35.7	33.8	35.7	38.0	41.4	41.9
Measured air flow rate (cm^3/sec)	3554	3296	4757	5361	4757	6396	5706	5704
Pressure 1 (D_h=1m, Z=2.5m) (kPa)	0.086	0.086	0.157	0.158	0.247	0.247	0.336	0.336
Pressure 2 (D_h=1m, Z=5m) (kPa)	1.256	1.295	2.404	2.434	3.707	3.706	4.809	4.713
Pressure 3 (D_h=1m, Z=7.5m) (kPa)	0.079	0.079	0.169	0.169	0.259	0.241	0.349	0.349
Pressure 4 (D_h=1m, Z=10m) (kPa)	0.059	0.059	0.112	0.095	0.059	0.041	0.041	0.041
Pressure 5 (D_h=2m, Z=2.5m) (kPa)	0.070	0.070	0.124	0.124	0.213	0.195	0.249	0.249
Pressure 6 (D_h=2m, Z=5m) (kPa)	0.589	0.589	1.078	1.097	1.737	1.736	2.313	2.282
Pressure 7 (D_h=2m, Z=7.5m) (kPa)	0.072	0.072	0.162	0.162	0.252	0.234	0.341	0.341
Pressure 8 (D_h=2m, Z=10m) (kPa)	0.049	0.049	0.085	0.085	0.121	0.121	0.175	0.193
Pressure 9 (D_h=4m, Z=2.5m) (kPa)	0.066	0.066	0.084	0.084	0.137	0.137	0.173	0.173
Pressure 10 (D_h=4m, Z=5m) (kPa)	0.182	0.164	0.362	0.362	0.561	0.561	0.741	0.741
Pressure 11 (D_h=4m, Z=7.5m) (kPa)	0.067	0.067	0.139	0.121	0.194	0.193	0.248	0.266
Pressure 12 (D_h=4m, Z=10m) (kPa)	0.049	0.031	0.085	0.085	0.103	0.103	0.174	0.192
Estimated anisotropy ratio (k_r/k_z)	3.6	4.9	4	3.6	3.51	3.53	3.5	3.61
Estimated horizontal permeability ($x10^{-12}$ m^2)	6.90	7.50	5.60	5.90	5.20	4.95	3.80	3.65

Table 3. Air permeability estimated from pneumatic testing data using AIR2D.

Injection air pressure (kPa)	5	5	10	10	15	15	20	20
Number of pressure transducers	12	12	12	12	12	12	12	12
Mass flow (g/sec)	4.41	4.09	6.10	6.91	9.07	8.57	7.90	7.73
Horizontal permeability ($x\ 10^{-12}$ m^2)	6.71	6.56	5.44	5.73	5.05	4.81	3.32	3.55
Vertical permeability ($x\ 10^{-12}$ m^2)	1.81	1.93	1.32	1.55	1.26	1.19	9.23	8.60
Anisotropy ratio (k_r/k_z)	3.70	3.40	4.12	3.70	4.01	4.04	3.60	4.13
Mean of error in pressure ($x\ 10^{-4}$)	9.32	4.11	2.43	2.79	5.08	5.22	6.76	6.54
Standard deviation in pressure ($x\ 10^{-4}$)	9.85	1.27	1.42	1.46	1.66	1.74	2.95	2.27

Table 4. Vertical permeability estimated from atmospheric pumping data.

z (m)	z/h	Amplitude ratio	λ	k ($x\ 10^{-12}$ m^2)
2.5	0.2232	0.9934	0.596610	0.93191
5.0	0.4464	0.9892	0.617777	0.86916
7.5	0.6696	0.9800	0.707350	0.66297
10.0	0.8929	0.9780	0.722725	0.63507

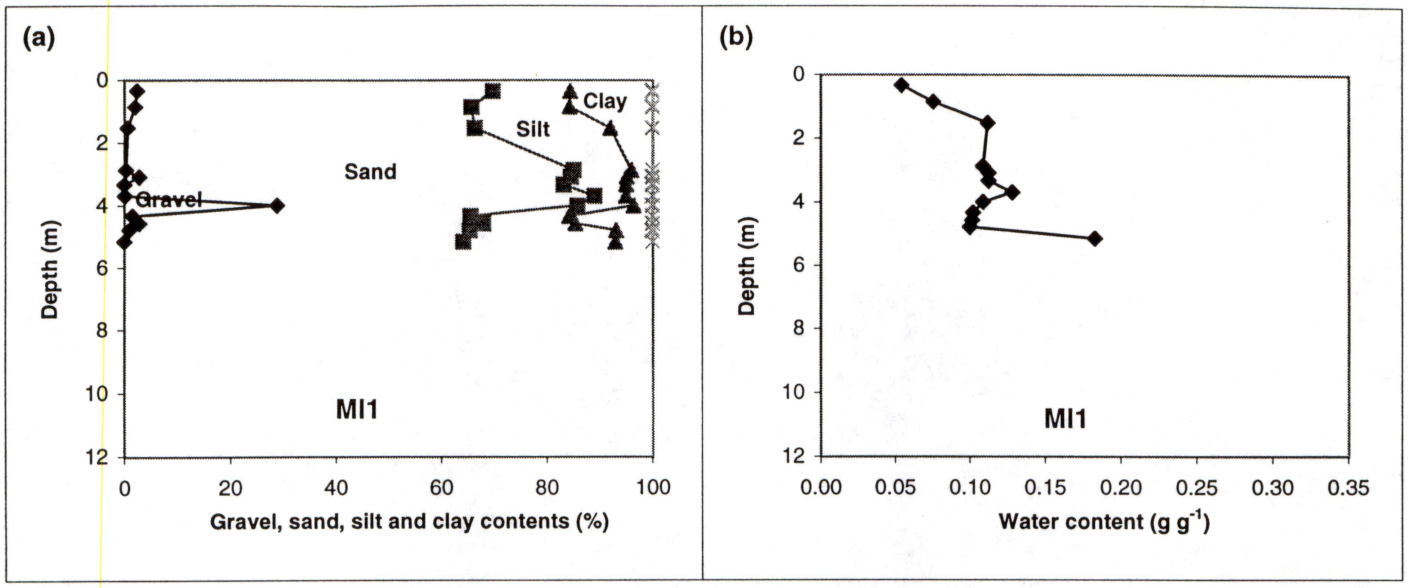

Figure 1. Soil texture and water content in samples from boreholes drilled for pneumatic testing (MI1, MP1, MP2, and MP4) and from boreholes drilled for monitoring atmospheric pumping (NAM1 and NAM2).

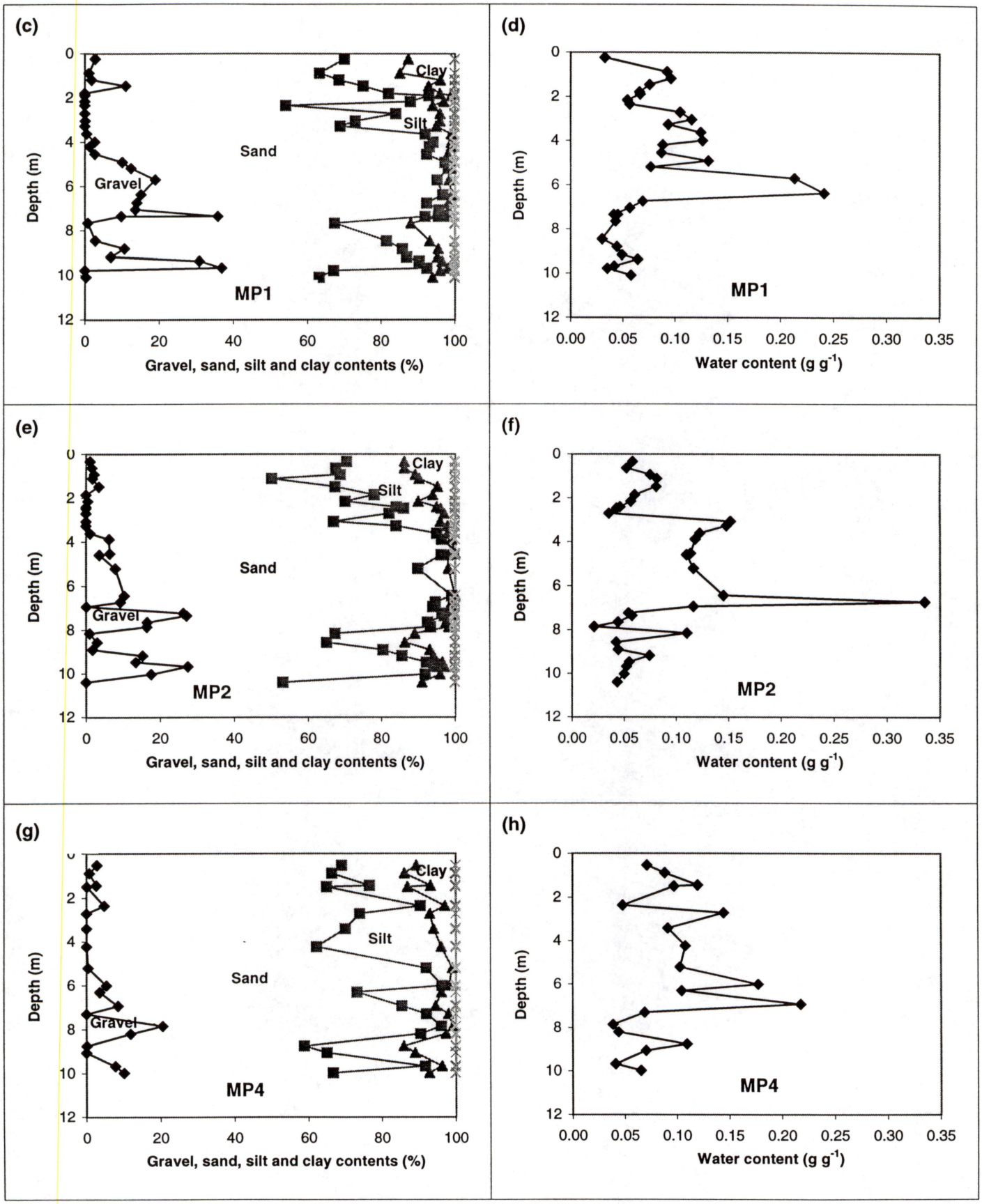

Figure 1. Soil texture and water content in samples from boreholes drilled for pneumatic testing (MI1, MP1, MP2, and MP4) and from boreholes drilled for monitoring atmospheric pumping (NAM1 and NAM2).

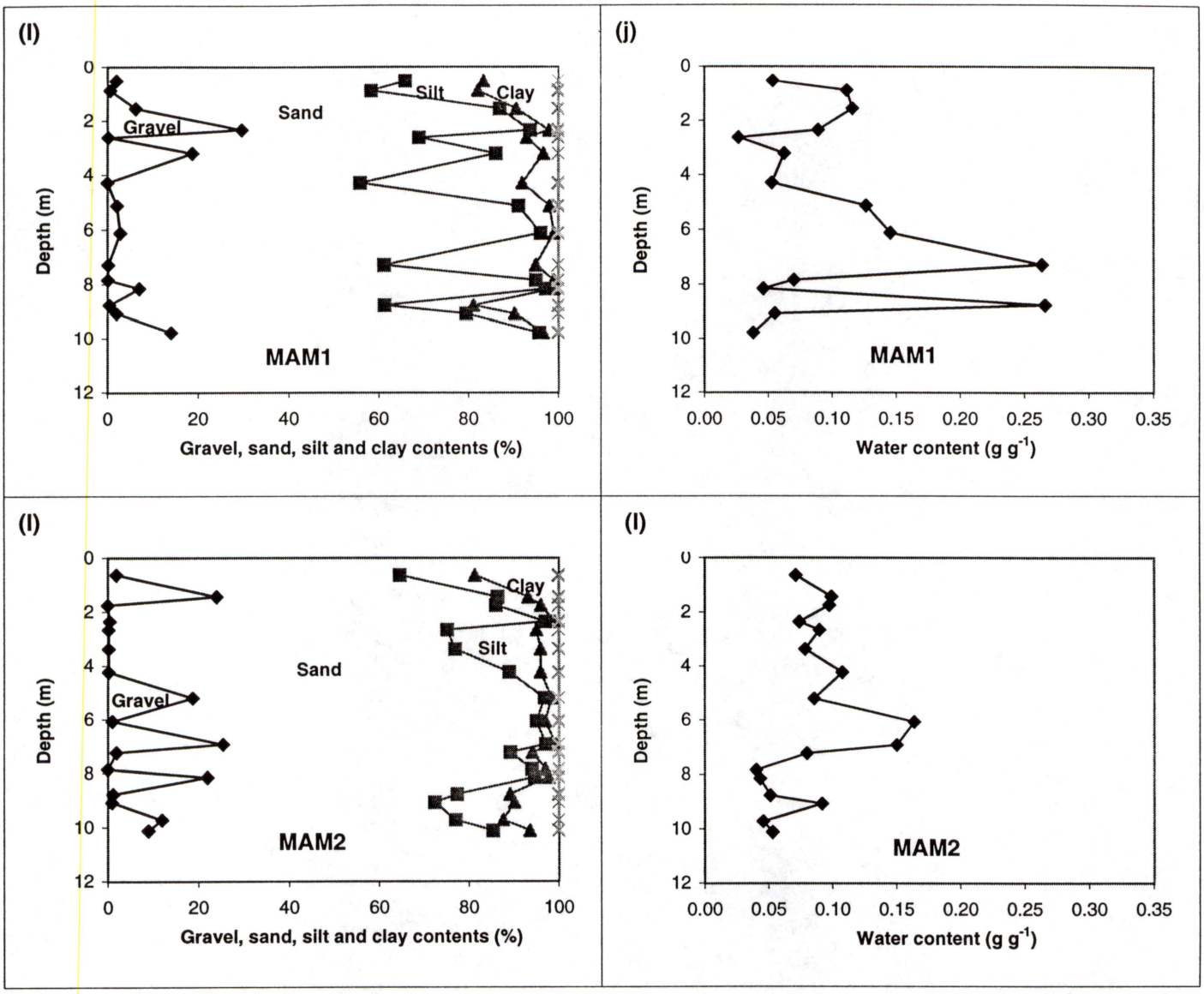

Figure 1. Soil texture and water content in samples from boreholes drilled for pneumatic testing (MI1, MP1, MP2, and MP4) and from boreholes drilled for monitoring atmospheric pumping (NAM1 and NAM2).

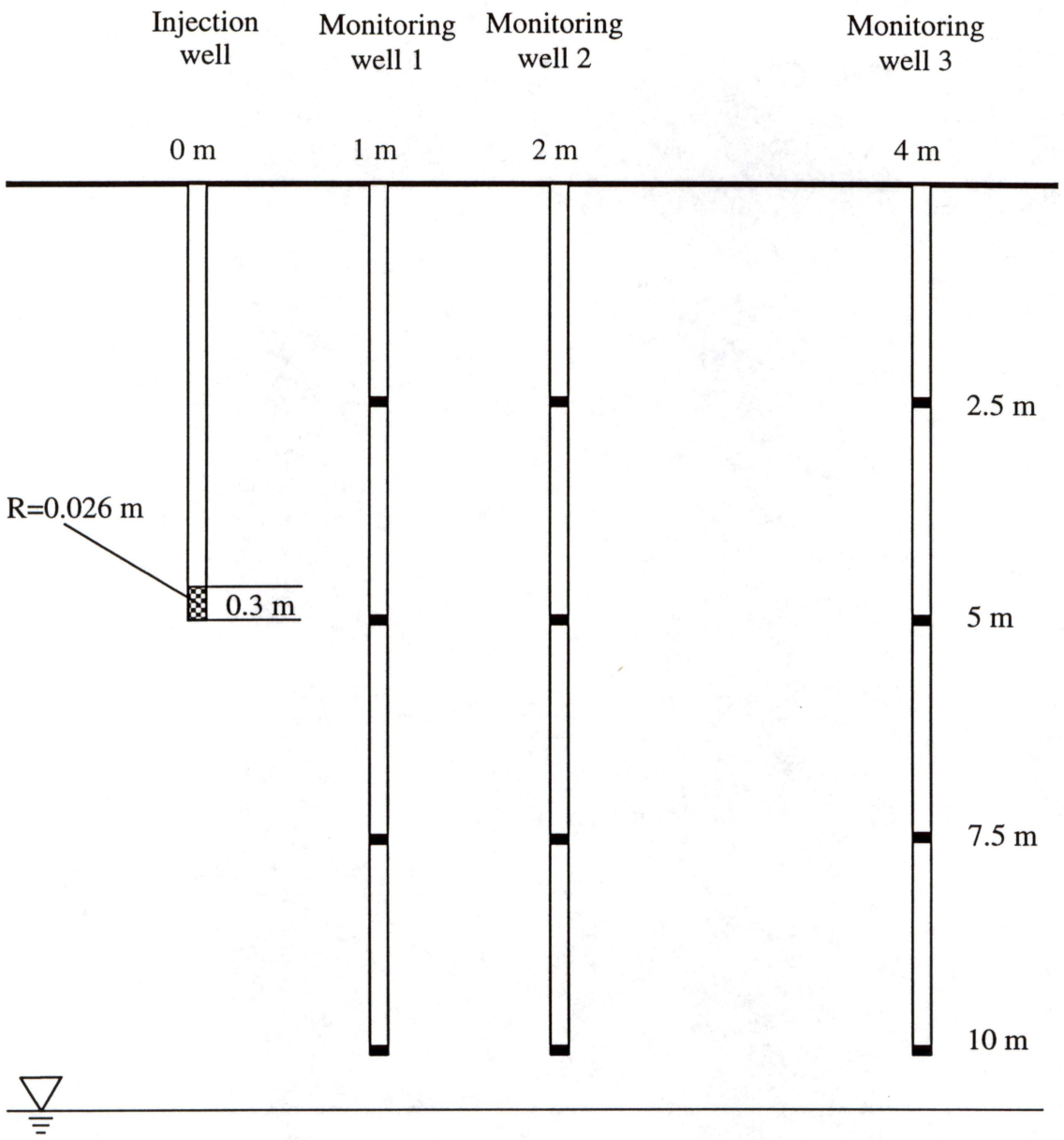

Figure 2. Cross section of wells used in pneumatic tests.

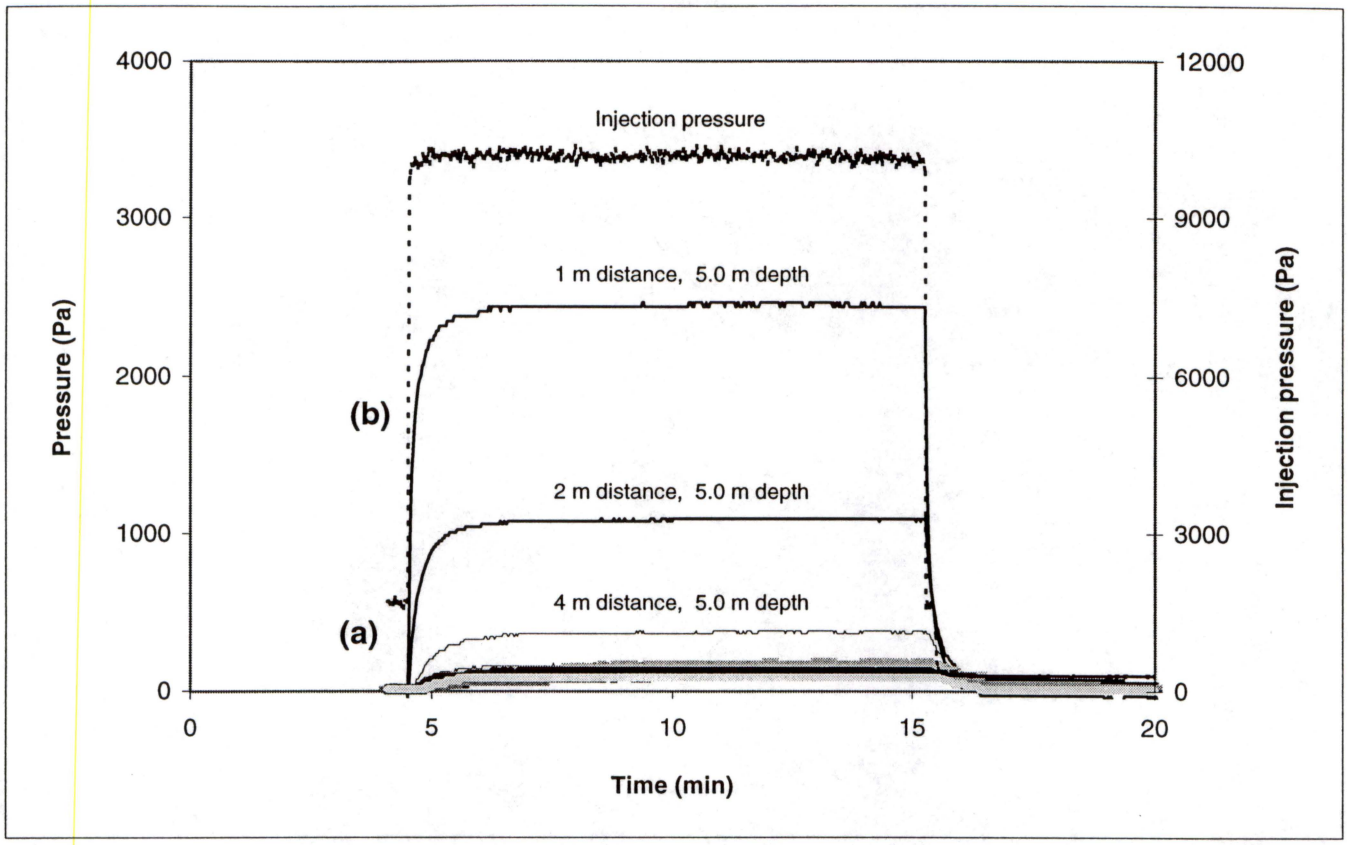

Figure 3. Injection pressure and pressures in monitoring wells during a typical pneumatic test.

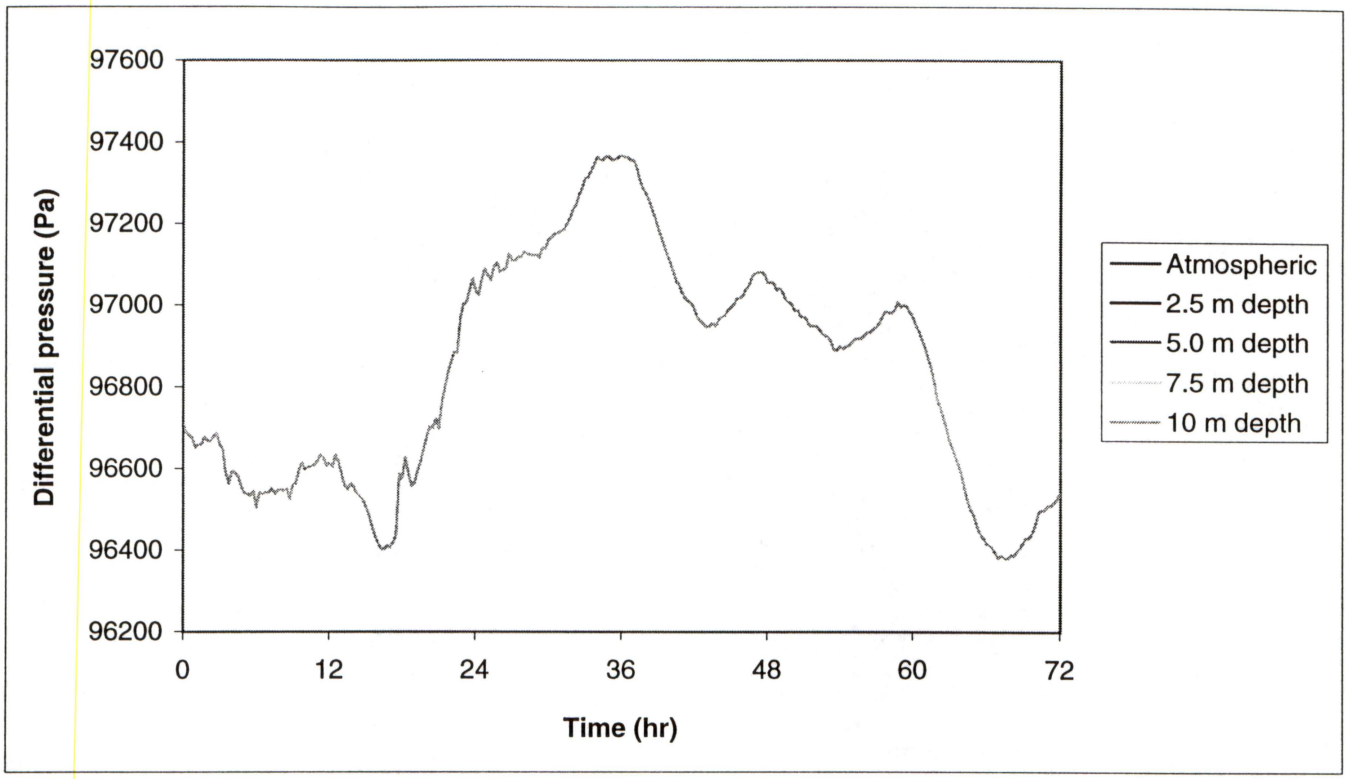

Figure 4. Surface and subsurface monitoring pressures in monitoring well MAM1 outside the irrigated plot from 9/25/98 through 9/27/98.

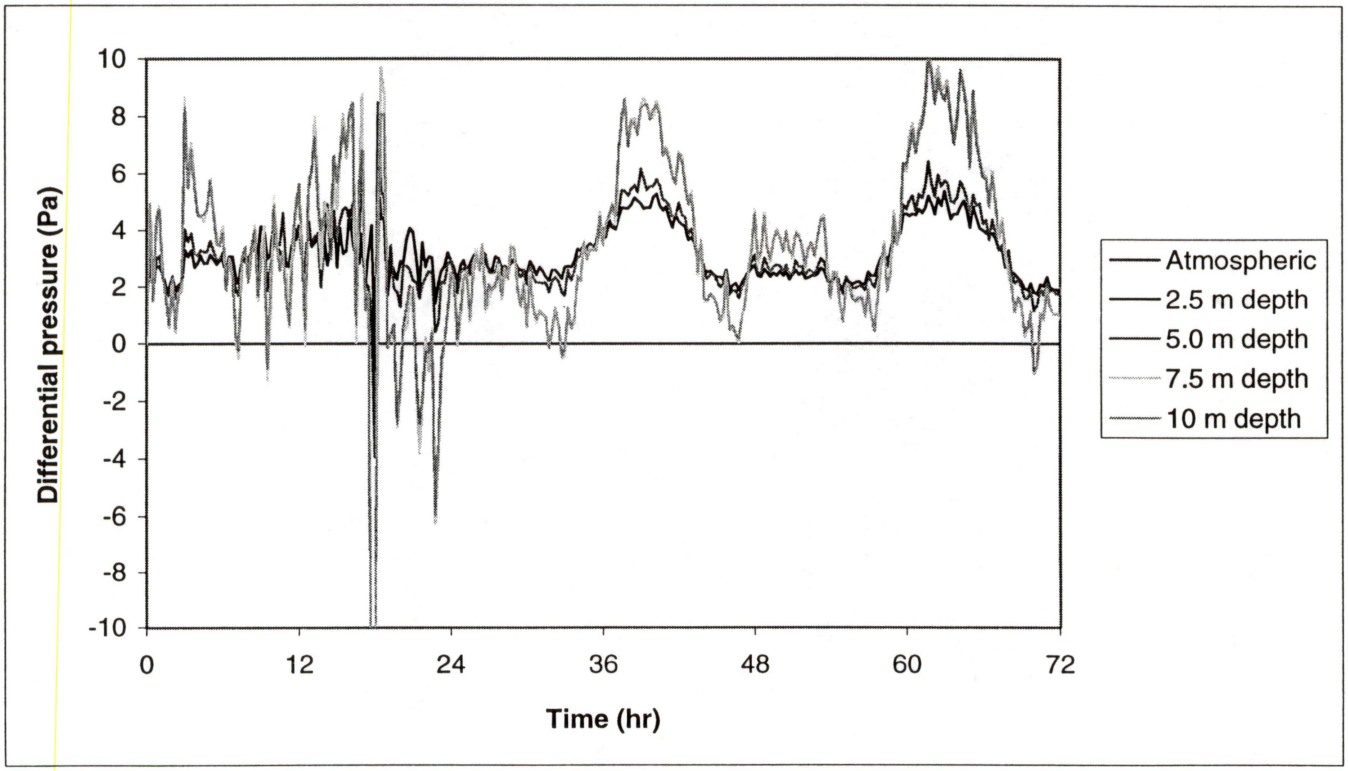

Figure 5. Differential pressure at different depths from 9/25/98 through 9/27/98.

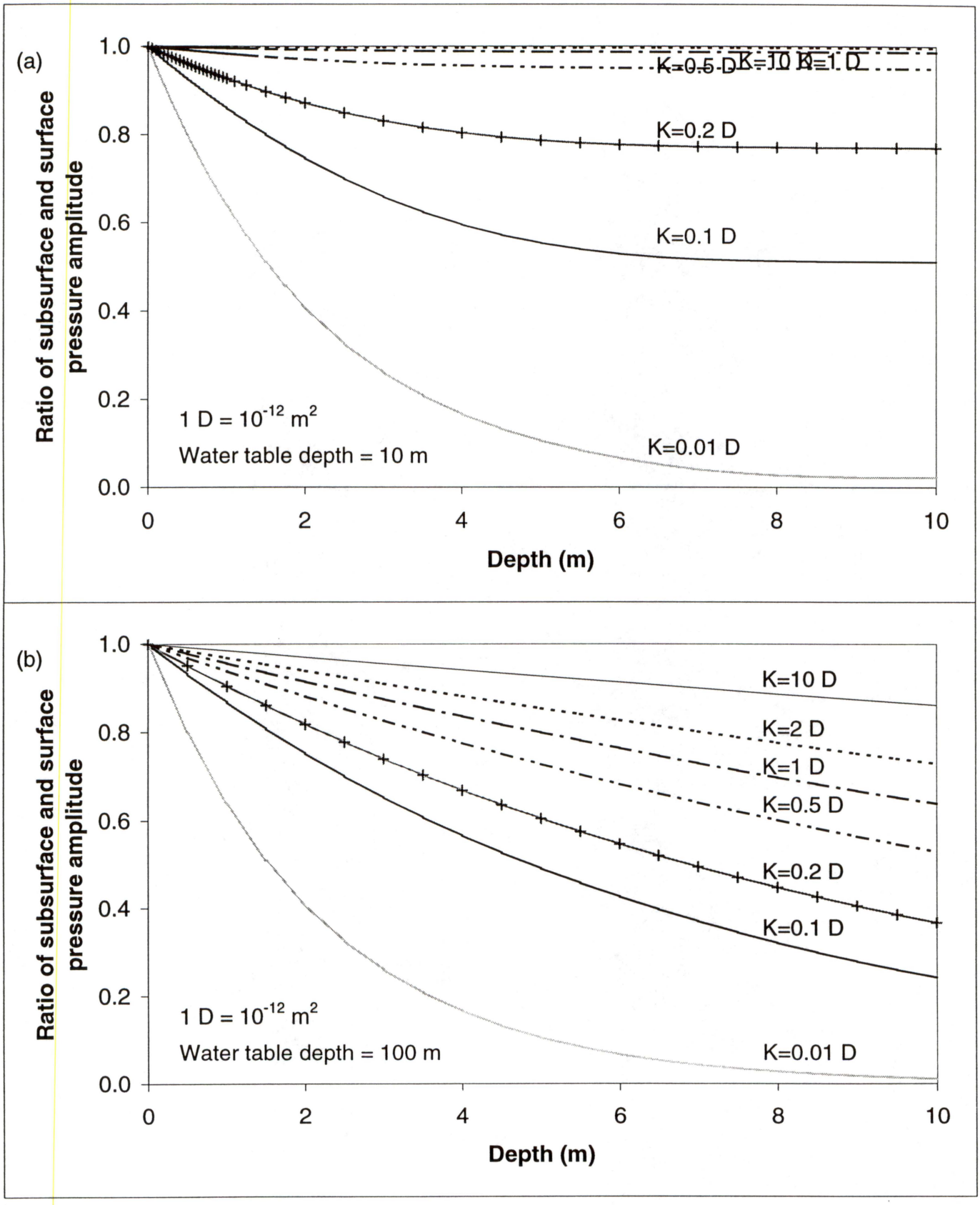

Figure 6. Sensitivity of the pressure amplitude ratio to variations in permeability (a) water table depth 10 m, (b) water table depth 100 m.